

Formation Mechanisms of Co-existence of α -Fe and Iron Oxides Nanoparticles Decorated on Carbon Nanofibers by a Simple Liquid Phase Adsorption-Thermal Oxidation

A. Alimin^{1*}, L. O. Kadidae¹, L. Agusu², L.O. Ahmad¹, S. J. Santosa³, A. Asria¹

¹ Department of Chemistry Universitas Halu Oleo Kampus Hijau Bumi Tridharma Anduonohu-Kendari 93232, Indonesia.

² Department of Physics Universitas Halu Oleo Kampus Hijau Bumi Tridharma Anduonohu-Kendari 93232, Indonesia.

³ Department of Chemistry Universitas Gadjah Mada-Yogyakarta, Indonesia.

Corresponding Author Email: aliminkim91@uho.ac.id

<https://doi.org/10.14447/jnmes.v25i3.a07>

ABSTRACT

Received: March 17-2022

Accepted: July 30-2022

Keywords:

Redox mechanisms, Lewis Acid-base mechanisms, carbon nanofibers, α -Fe nanoparticles, iron oxides, liquid-phase adsorption

We propose formation mechanisms of co-existence of α -Fe and iron oxides nanoparticles decorated on CNFs. The α -Fe nanoparticles are produced via oxidation-reduction mechanisms, which occur in liquid phase adsorption (LPA) assisted by ultrasonic energy, while α -Fe₂O₃ nanoparticles are thermally formed through mechanisms of Lewis acid-base. In addition, Fe₃O₄ is thermally formed by reducing Fe₂O₃ by CNFs. Liquid phase adsorption assisted by ultrasonic energy under ambient temperature using Fe(NO₃)₃•9H₂O as a precursor of iron oxides and α -Fe has been applied. Then, as prepared, Fe(III)@CNFs were thermally calcined at 573 K under air atmosphere in various holding times ranging from 0.5 to 2 h. XRD data confirmed that α -Fe₂O₃ and Fe₃O₄ had been successfully grown onto CNFs.

Moreover, the presence of the iron oxides and iron nanoparticles was studied by the SEM-EDX technique. The iron oxide nanoparticles appeared after a heating period of 0.5h. However, at a holding time of 0.5 h, we found an exciting and unexpected phenomenon where oxygen content is zero percent while Fe is 0.23 wt %. It implies that α -Fe nanoparticles were formed earlier than α -Fe₂O₃ and Fe₃O₄ as the proposed mechanisms. Formation mechanisms of iron and its oxides such as α -Fe₂O₃ and Fe₃O₄ decorated on CNFs through liquid-phase adsorption followed by thermally treatment technique in this work is expected to give significant contribution in the field of nanocomposite materials, especially for anode materials based on iron oxides.

1. INTRODUCTION

Production of iron or iron oxide nanoparticles [1-18] and loading those nanoparticles on nanocarbon has been intensively studied [19-22]. The nanoparticles and their composite with nanocarbon have been widely applied in nanosciences and nanotechnology fields such as energy storage [23-25], electrochemical [26-27], and sensing technology [28,29]. Synthesis and decoration of iron or iron oxides onto nanocarbon lead to the creation of a principally new type of functional nanostructures having unique chemical and physical properties. In the last decade, one type of nanocarbon that has been paid attention to by the researcher community is carbon nanofiber (CNFs), which is decorated by iron or their oxides [19-22]. There are two routes to functionalize nanocarbons, one is the gas route phase [30], and the other is the liquid phase route followed by heating under air [19,31]. Among these, the liquid phase route has been intensively used for loading metal nanoparticles on nanocarbon because of its simple treatment, relatively high homogeneity, and the distribution of nanoparticles on nanocarbon is relatively uniform. For example, Alimin *et al.* [19] prepared a nanocomposite of α -Fe₂O₃/CNFs/PET for lithium-ion batteries anode by liquid-phase adsorption (LPA)

followed by calcination technique. Palen *et al.* [31] produced Fe nanoparticles into nanocarbon through two stages. i.e., liquid phase route accompanied by heating treatment under an air atmosphere at 593 K to decompose the FeCl₃ to iron and chlorine. However, they used the over-saturated solution of iron (III) chloride as a precursor of the nanoparticles. In the recent past, iron oxide production on carbon nanofiber was done by employing electrospinning methods followed by a physical or chemical technique. Pai *et al.* [20] reported in situ grown iron oxides on carbon nanofibers through electrospinning followed by an in situ electrochemical technique. Cho *et al.* [21] synthesized bubble-nanorod-structured Fe₂O₃-carbon nanofibers through several stages. Composite nanofibers consisting of iron acetylacetonate [Fe(acac)₃] and polyacrylonitrile (PAN) were prepared by the electrospinning process. Post-treatment of the electrospun precursor nanofibers at relatively high temperature, i.e., 500 °C under H₂/Ar mixture gas atmosphere, produced amorphous FeOx-carbon composite nanofibers. The carbonization of PAN and the decomposition of iron acetylacetonate produced FeOx-carbon composite nanofibers. The subsequent post-treatment of the FeOx_carbon composite nanofibers at 300 °C under air atmosphere produced the bubble-nanorod-structured Fe₂O₃-C composite nanofiber. Reduction of FeOx crystals

surrounded by the carbon matrix into Fe metal occurred during the post-treatment under air atmosphere. Cao *et al.* [22] synthesized core-shell $\alpha\text{-Fe}_2\text{O}_3\text{@NiO}$ nanofibers using the coaxial electrospinning method and calcination procedure. Based on the above description, it can be stated that even though various techniques have been applied for producing the nanoparticles loaded on nanocarbons, most of them still exhibit advantages and disadvantages. Thus, growing iron oxide and iron nanoparticles on nanocarbon is still an interesting study.

Regarding the production of $\alpha\text{-Fe}$ nanoparticles on nanocarbon, Palen *et al.* [31] have produced $\alpha\text{-Fe}$ nanoparticles on nanocarbon via two stages, i.e., liquid and heating treatment. However, in our work, we have successfully produced $\alpha\text{-Fe}$ nanoparticles on CNFs through one step, i.e., liquid phase adsorption (LPA). To the best of our knowledge, reduction of ions Fe^{3+} to $\alpha\text{-Fe}$ nanoparticles on carbon nanofiber (CNFs) via liquid-phase adsorption (LPA) technique has never been reported. Hence, in the present work, we produced $\alpha\text{-Fe}$ nanoparticles on carbon nanofiber (CNFs) using a liquid-phase adsorption route under ambient temperature where $\text{Fe}(\text{NO}_3)_3 \cdot 9\text{H}_2\text{O}$ as a precursor of the nanoparticles. Then, as prepared, $\text{Fe}(\text{III})\text{@CNFs}$ were calcined at 573 K in various holding times ranging from 0.5 to 2 h to produce iron oxides nanoparticles. In the present work, the formation mechanisms of $\alpha\text{-Fe}$ and iron oxides on CNFs were also proposed. Based on the literature review, not many researchers are concerned about studying the formation mechanisms of co-existence of $\alpha\text{-Fe}$ and iron oxides nanoparticles on carbon nanofibers. Most of the studies were focused on the formation mechanisms of iron oxides nanoparticles [1-18,32], while formation mechanisms of iron oxide on CNFs, as reported by Mu *et al.* [33], just focused on the physical mechanisms of growth of the nanoparticles on CNFs. In the present work, we studied the reaction mechanism of the production of nanoparticles on CNFs as the main objective of this study. Next, this work contributes to the elucidation of the effect of ultrasonic and thermal energies on the production mechanisms of iron and its oxides on CNFs. Understanding the correlation among formation mechanisms, iron, and its oxides species, and types of the employed energy enables to fulfillment of one of the purposes of this study, i.e., production of iron nanoparticles and its oxides on CNFs via liquid-phase adsorption using ultrasonic energy accompanied by calcination under air atmosphere.

2. EXPERIMENTAL METHOD

2.1 Chemicals

All chemicals used in this study were of analytical grade with high purity. $\text{Fe}(\text{NO}_3)_3 \cdot 9\text{H}_2\text{O}$ 99.5 wt% (E. Merck), Carbon nanofibers (CNFs) we purchased from the sigma Aldrich, ethanol 99.5 wt% (J.T.Baker), Whatman Millipore 0.45 μm .

2.2 Production of $\alpha\text{-Fe}$ and iron oxides nanoparticles grown on carbon nanofibers

The $\alpha\text{-Fe}$ and iron oxides nanoparticles decorated on carbon nanofibers were performed using simple liquid-phase adsorption (LPA) and sequential LPA-thermal oxidation technique. Prior to calcination of $\text{Fe}(\text{III})\text{-CNFs}$, we conducted doping of $\text{Fe}(\text{NO}_3)_3 \cdot 9\text{H}_2\text{O}$ solution into CNFs using a similar technique with our previous work

[19]. Briefly, CNFs were dipped in $\text{Fe}(\text{NO}_3)_3 \cdot 9\text{H}_2\text{O}$ solution containing water, and it was then dispersed ultrasonically by ultrasound apparatus of 53 kHz for 30 minutes at ambient temperature. As-prepared CNFs were then filtered using a Millipore porous filter (0.45 μm). The treated samples denoted as $\text{Fe}(\text{III})\text{@CNFs}$ were then calcined under an air atmosphere at 573 K in various holding times of 0.5, 1.0, 1.5, 2.0, and 2.5 hours to obtain Fe oxide nanoparticles doped on CNFs. SEM-EDX then characterized the morphology and chemical composition of the nanoparticles. XRD technique was used to identify the crystal structure of the iron oxides.

3. RESULTS AND DISCUSSION

3.1. Characterization of co-existence of $\alpha\text{-Fe}$ and iron oxides nanoparticles on CNFs

Figure 1 shows XRD patterns of pristine CNFs(a) and $\text{Fe}(\text{III})\text{@CNFs}$ (b). Figure 1(b) can be interpreted as follow; diffraction peaks located at $2\theta = 33.2^\circ$, 39.3° , and 69.6° are coincided well with the value of JCPDS card no. 33-0664. Those peaks are associated with reflections of the crystallographic planes of $\alpha\text{-Fe}_2\text{O}_3$, i.e., (104), (006), and (208), respectively. Other peaks at 37.1° and 57.0° are matched by JCPDS card no. 06-0696 (curve b), which could be well indexed to the phase of Fe_3O_4 , i.e., (222), and (511). The last diffraction peaks at $2\theta = 44.7^\circ$ and 65.0° correspond to diffraction spectra of $\alpha\text{-Fe}$ (JCPDS card no. 06-0696) with crystallographic planes of (110) and (200). These results are in good agreement with the work of Zhang *et al.* [18].

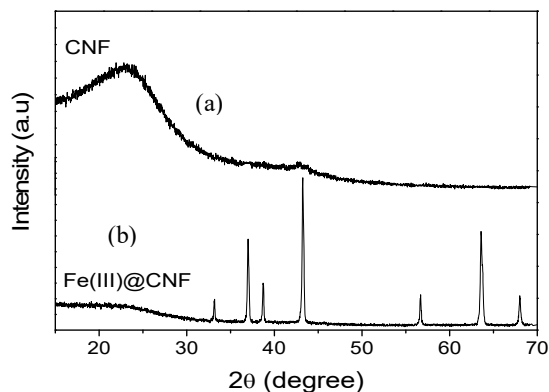


Figure 1. XRD patterns of pristine CNFs (a) and LPA-Oxidation Thermal of $\text{Fe}(\text{III})\text{@CNF}$

EDX spectra of pristine CNFs and $\text{Fe}(\text{III})\text{@CNFs}$ are shown in Fig. 2. The principal investigated elements appeared on EDX data are tabulated in Table 1.

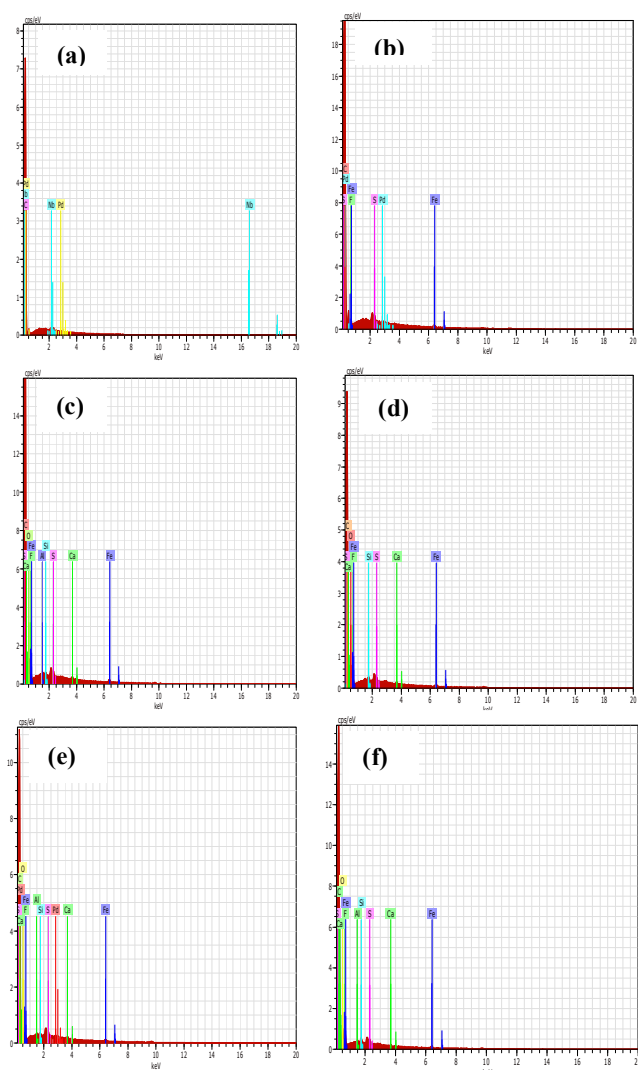


Figure 2. EDX spectra of pristine CNFs and calcined Fe(III)@CNFs : (a) Pristine CNFs, (b) calcination for 0.5 h, (c) calcination for 1h, (d) calcination for 1.5 h, (e) calcination for 2 h and (f) calcination for 2.5 h

Table. 1 EDX data of Fe, O, and C compositions in Fe (III)-doped CNFs heated at 573 K

Calcination time (hour)	Elemental composition (wt %)		
	Fe	O	C
0.5	0.23	0	97.10
1.0	0.15	12.78	84.78
1.5	0.18	13.69	83.33
2.0	0.20	10.36	87.39
2.5	0.14	11.77	83.42

EDX data shows that the presence of O element when heating periods above 0.5 h strongly indicates Fe oxide formation such as Fe_3O_4 and Fe_2O_3 as indicated by XRD patterns. In addition, the decrease of carbon content above a heating period of 0.5 h implies that the iron oxides have been formed. According to Cho *et al.* [34], FeO_x can react with C giving $\text{CO}_{(g)}$, and therefore the carbon content tends to decrease by heating under a specific temperature and calcination time. The formation of the oxides is strongly

affected by temperature and time calcinations. Fe_3O_4 and Fe_2O_3 were produced on CNFs above 0.5 h under relatively low temperatures (573 K). Monazam *et al.* [6] reported the formation of Fe_3O_4 and Fe_2O_3 under relatively high temperatures ranging from 1,023 to 1,173 K.

Based on EDX data (Table 1 and Figure 2), it can be seen that the spectrum of Fe is observed with the highest composition of 0.23 wt % while O is not (0 wt %), suggesting that α -Fe nanoparticles are formed early stage while iron oxides are not. The production of Fe nanoparticles in a relatively short period is an exciting and unexpected phenomenon in this study. Based on this phenomenon, presumably α -Fe nanoparticles have been produced by liquid-phase adsorption during the interaction between CNFs and Fe (III) ions. Therefore, in this study, we proposed the mechanisms of formation of α - Fe_2O_3 and α -Fe that will be discussed in section 3.2.

Figures 3(a) and 3(b-f) show SEM images of pristine CNFs and Fe(III)@CNFs heated at 573 K in various calcination times, respectively.

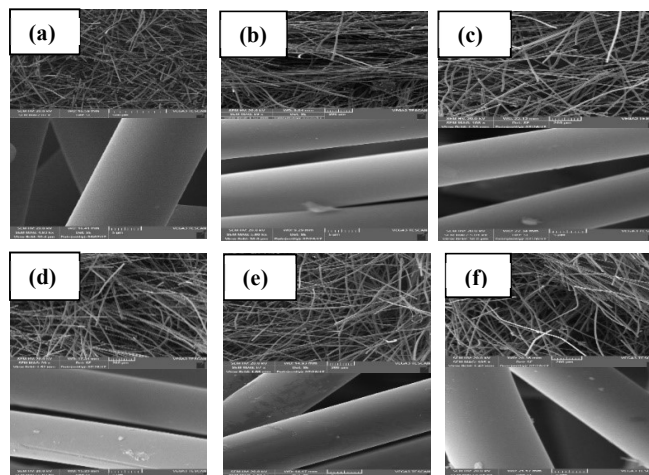


Figure 3. SEM images of pristine CNFs and calcined Fe(III)@CNFs comparing low magnification (L) in upper part and high magnification (H) in lower part: (a) Pristine CNFs (L=87x, H= 4.9kx), (b) calcination for 0.5 h (L=99x, H= 5.0 kx), (c) calcination for 1h (L=108x, H= 5.01 kx), (d) calcination for 1.5 h (L=99x, H= 5.03 kx), (e) calcination for 2 h (L=97x, H= 5.01 kx) and (f) calcination for 2.5 h (L=105x, H= 5.01 kx)

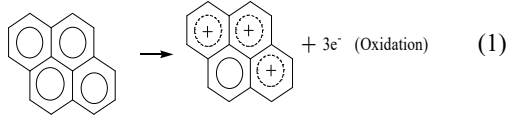
some relatively large particles, as shown in Figure 3(b-f). On the contrary, the nanoparticles are not found on the external surface of pristine CNFs (Fig. 3-a). The presence of particles on the external surface of CNFs indicates that Fe (III) metal ions have successfully been doped onto CNFs through liquid-phase adsorption. Those particles might be identified as Fe oxides formed after heating at 573 K in various holding times. It is reasonable that an oxidation process should occur during calcination under an air atmosphere, and Fe oxides were then produced.

3.2. Mechanisms of α -Fe and iron oxides are grown on CNFs

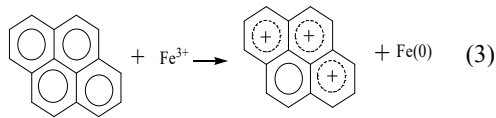
The formation mechanisms of α -Fe and iron oxides on CNFs were studied by XRD patterns (Fig. 1) and EDX data

(Fig. 2 and Table 1). The XRD patterns and EDX data show that α -Fe, Fe_3O_4 , and Fe_2O_3 were produced on CNFs.

There are three possibilities of mechanisms that we proposed in this study. One is redox mechanisms dealing with the formation of α -Fe that take place at liquid phase adsorption assisted by ultrasonic energy. The proposed mechanisms are written as follow:

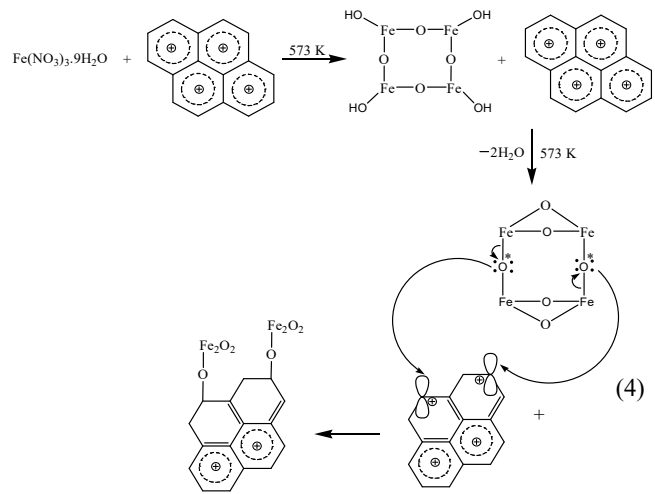


The overall reaction can be written as follow;

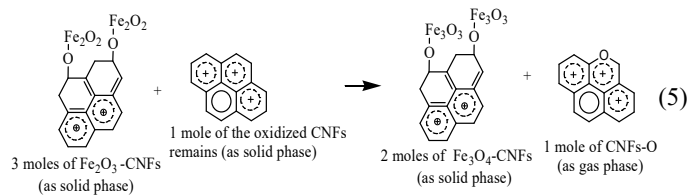


In this case, CNFs can act as reducing agents while Fe^{3+} ions act as an oxidizing agent, and therefore, CNFs might play an essential role in reducing $\text{Fe}(\text{III})$ ions into $\text{Fe} (0)$. The role of CNFs as a reduction agent of a transition metal ion was also found in the production of silver nanoparticles on nanocarbon where π -bond in the nanocarbon played an essential role for growing the metal nanoparticles [35]. In general, the formation of Fe nanoparticles takes place at a relatively higher temperature, such as ~ 700 K under inert gas atmosphere [28] and under air atmosphere at 593 K for one h [31] and 973 K for three h [36]. In our work, however, we found that transformation of $\text{Fe} (\text{III})$ ions into Fe nanoparticles occurred at a relatively low temperature of 573 K for 0.5 h, which was relatively shorter than the calcination time of other groups.

The second mechanism is that reaction between the remained $\text{Fe}(\text{NO}_3)_3 \cdot 9\text{H}_2\text{O}$ and the oxidized CNFs resulted from the former mechanisms giving iron oxide of Fe_2O_3 . The mechanisms occurred when the $\text{Fe}(\text{NO}_3)_3 \cdot 9\text{H}_2\text{O}$ doped onto the oxidized CNFs was calcined at 573 K at above 0.5 h. According to the thermal decomposition mechanisms of iron nitrate salt proposed by Melnikov *et al.* [37], only a tetranuclear skeleton $\text{Fe}_4\text{O}_4(\text{OH})_4$ remains upon completion of denitrification. Finally, this cyclic oxyhydroxide loses 2 moles of the remaining water, providing an unstable dimer of ferric oxide. By referring to those mechanisms, we propose thermal mechanisms of the formation of Fe_2O_3 on CNFs. Briefly, the mechanisms can be ascribed as follow; when the skeleton $\text{Fe}_4\text{O}_4(\text{OH})_4$ interacts with the oxidized CNFs under 573 K, it releases two water molecules giving an unstable dimer of ferric oxide. Then, each O atom signed O^* in ferric oxide dimer interacts coordinately with C^+ in CNFs, giving 2 moles of ferric oxide bounded coordinately in CNFs structure. In this case, a lone pair electron on O^* in ferric oxide dimer is donated to C^+ in CNFs, and then coordination bonds between C atoms of CNFs and O atoms of Fe_2O_3 are formed. Briefly, the mechanisms can be described as Lewis acid-base reaction that is written in the following mechanisms;



The third mechanism is the formation of Fe_3O_4 that might be produced by a redox reaction between the remained CNFs and Fe_2O_3 bound on CNFs. Kawana *et al.* [38] suggested that carbon can reduce Fe_2O_3 to be Fe_3O_4 accompanied by the formation of CO gas. Based on the redox mechanism suggested by Kawanari *et al.*, then presumably that 3 moles of Fe_2O_3 react with 1 mole of the oxidized CNFs, it should then give 2 moles of Fe_3O_4 -CNFs accompanied by the formation of 1 mole of CNFs-O gas (eq.5). It means that Fe_2O_3 bound on CNFs are reduced to be Fe_3O_4 . However, both Fe_2O_3 and Fe_3O_4 are observed on XRD patterns. It suggests that Fe_2O_3 found on XRD patterns are Fe_2O_3 remains that are not consumed in the redox reaction. Hence, we propose the mechanism as follows;



Theoretically, the existence of carbon can reduce Fe_3O_4 to be FeO [36]. Nevertheless, in our work, the FeO was not produced. It agrees with the XRD patterns in Figure 1, which indicates that crystal planes of FeO were not formed.

4. CONCLUSIONS

We succeeded produced α -Fe, α - Fe_2O_3 , and Fe_3O_4 nanoparticles with a Simple Liquid Phase Adsorption (LPA) followed by Thermal Oxidation through three steps of mechanisms. The first step is the ultrasonic formation of α -Fe nanoparticles from Fe^{3+} ions in the liquid phase via oxidation-reduction mechanisms. The second is the thermal production of α - Fe_2O_3 nanoparticles through Lewis acid-base mechanisms. The last step is the thermal formation of Fe_3O_4 via reduction of α - Fe_2O_3 by CNFs. We found an exciting and unexpected phenomenon in which Fe nanoparticles were produced onto CNFs at an earlier calcination time of 0.5 h. Formation α -Fe nanoparticles might occur during the interaction between Fe^{3+} ions and CNFs in the liquid phase assisted by ultrasonic energy as first step mechanisms. α -

Fe₂O₃ and Fe₃O₄ were formed at calcination time above 0.5 h through the second and third pathways.

ACKNOWLEDGMENT

The authors thank the Directorate of Research and Community Service-The Ministry of Research, Technology and Higher Education of the Republic of Indonesia for funding this work through the Research Grant for Applied Product # 065/ADD/SP2H/LT/DRPM/VIII

REFERENCES

- [1] Rasheed, R.T., Al-Algawi, S.D., Kareem H.H., and Mansoor, H.S. (2018). Preparation and Characterization of Hematite Iron Oxide (α -Fe₂O₃) by Sol-Gel Method. *Chemical Sciences Journal*. 9(4). DOI: 10.4172/2150-3494.1000197
- [2] Cho, J.S., Y.J., Lee, J.H., and Kang, Y.C. (2012). Design and Synthesis of Micron-Sized Spherical Aggregates Composed of Hollow Fe₂O₃ Nanospheres for Use in Lithium-Ion Batteries. *Nanoscale*. www.rsc.org/nanoscale. DOI:10.1039/C5NR01391G
- [3] Besenhard, M.O., LaGrow, A.P., Hodzic, A., Kriechbaum, M., Panariello, L., Bais, G., Loizou, K., Damilos, S., Cruz, M.M., Thanh, N.T.K., Gavriilidis, A. (2020). Co-precipitation Synthesis of Stable Iron Oxide Nanoparticles with NaOH: New Insights and Continuous Production via Flow Chemistry. *Chemical Engineering Journal*. https://doi.org/10.1016/j.cej.2020.125740
- [4] Chirita, M., Kiss, M.L., Ieta, A., Ercuta, Aurel., and Grozescu, I. (2015). Synthesis of Micrometric Single-Crystalline Magnetite with Superparamagnetic Properties for Biomedical Applications. *NSTI-Nanotech*. www.nsti.org, ISBN 978-1-4822-0581-7 Vol. 1
- [5] Schwaminger, S.P., Syhr, C., and Berensmeier, S. (2020). Controlled Synthesis of Magnetic Iron Oxide Nanoparticles: Magnetite or Maghemite?. *Crystals*. 10(214). Doi:10.3390/cryst10030214
- [6] Monazam, E. R., Breault, R.W., and Siriwardane, R. (2014). Kinetics of Magnetite (Fe₃O₄) Oxidation to Hematite (Fe₂O₃) in Air for Chemical Looping Combustion. *Industrial & Engineering Chemistry Research*. dx.doi.org/10.1021/ie501536s. 53. 13320–13328
- [7] Koo, K.N., Ismail, A.F., Othman, M.H.D., Rahman, M.A, Sheng, T.Z . (2019). Preparation and Characterization of Superparamagnetic Magnetite (Fe₃O₄) Nanoparticles: A short Review. *Malaysian Journal of Fundamental and Applied Sciences*. 15(10): 23-31
- [8] Lina, C.C., Lee, C.Y. (2019). Adsorption of Ciprofloxacin in Water Using Fe₃O₄ Nanoparticles Formed at Low Temperature and High Reactant Concentrations in a Rotating Packed Bed with Co-precipitation. *Materials Chemistry and Physics*. https://doi.org/10.1016/j.matchemphys.2019.122049
- [9] Roca, A.G., Gutiérrez, L., Gavilán, H., Brollo, M.E. F., Verdager, S.V., Morales, M. del Puerto. (2019). Design Strategies for Shape-controlled Magnetic Iron Oxide Nanoparticles. *Advanced Drug Delivery Reviews* 138. 68–104.
- [10] Salviano, L.B., Cardoso, T.M. da Silva., Silva, G. C., Maria Dantas, S.S., Ferreira, A. de Mello. (2018). Microstructural Assessment of Magnetite Nanoparticles (Fe₃O₄) Obtained by Chemical. *Materials Research*. 21(2). DOI: http://dx.doi.org/10.1590/1980-5373-MR-2017-0764
- [11] Pawara, R.C., Um, J. H., Kang, S, Yoon,W.S., Choe. H., Lee, C.S. (2017). Solvent-Polarity-Induced Hematite (α -Fe₂O₃) Nanostructures for Lithium-Ion Battery and Photoelectron Chemical Applications. *Electrochimica Acta*. 245. 643–653. http://dx.doi.org/10.1016/j.electacta.2017.05.070
- [12] Cursaru, L.M., Piticescu, R.M., Dragut, D.V., Tudor, I.A., Kuncser, V., Iacob, N., and Stoiciu, F. (2020). The Influence of Synthesis Parameters on Structural. *Nanomaterials*. 10(85). doi:10.3390/nano10010085
- [13] Takai, Z.I., Mustafa, M.K., Asman, S., and Sekak, K.A. (2019). Preparation and Characterization of Magnetite (Fe₃O₄) Nanoparticles by Sol-Gel Method. *International Journal of Nanoelectronics and Materials*. 12(1): 37-46
- [14] Nene, A.J., Takahashi, M., Somani, P.R. (2016). Fe₃O₄ and Fe Nanoparticles by Chemical Reduction of Fe(acac)₃ by Ascorbic Acid: Role of Water. *World Journal of Nano Science and Engineering*. http://dx.doi.org/10.4236/wjnse.2016.61002
- [15] Rodríguez, C.T., García, J.C., Sánchez, L.T., López, A., Dief, A.M.A., Costa, A., Elbaile, L., Crespo, R.D., Garitaonandia, J.S., Lastra, E., García, J.A., and Alonso, F.J.G. (2019). A Simple and Reliable Synthesis of Superparamagnetic Magnetite Nanoparticles by Thermal Decomposition of Fe(acac)₃. *Journal of Nanomaterials*. https://doi.org/10.1155/2019/2464010
- [16] Noqta, O.A., Aziz. A.A., Usman, I.A., Bououdina, M. (2019). Recent Advances in Iron Oxide Nanoparticles (IONPs): Synthesis and Surface Modification for Biomedical Applications. *Journal of Superconductivity and Novel Magnetism*. 32. 779–795. https://doi.org/10.1007/s10948-018-4939-6
- [17] Nguyen, M.D., Tran, H.V., Xu, S., and Lee, T.R. (2021). Fe₃O₄ Nanoparticles: Structures, Synthesis, Magnetic Properties, Surface Functionalization, and Emerging Applications. *Applied Sciences*. 11. 11301. https://doi.org/10.3390/app112311301
- [18] Zhang, S., Wu, W., Xiao, X., Zhou, J., Ren, F., Jiang, C. (2011). Preparation and characterization of spindle-like Fe₃O₄ mesoporous nanoparticles. *Nanoscale Research Letters*.(6):89.http://www.nanoscalereslett.com/content/6/1/89
- [19] Alimin, Amrin, Hasrudin, Hamid, I.A., Nurdin, M., Aba, L., Zamrun, M., Agus. L. (2019). Synthesis of Lithium-Ion Batteries Anode Based on Fe Oxide-Carbon Nanofibers/poly (Ethylene Terephthalate) Nanocomposite. *IOP Conf. Series: Journal of Physics: Conf. Series* 1153 (2019) 012094. doi:10.1088/1742-6596/1153/1/012094
- [20] Pai, R., Singh, A., Simotwo, S., and Kalra, V. (2018). In Situ Grown Iron Oxides on Carbon Nanofibers as Freestanding Anodes in Aqueous Supercapacitors. *Advanced Engineering Materials*. DOI: 10.1002/adem.201701116
- [21] Cho, J.S., Hong, Y.J., and Kang, Y.C. (2015). Design and Synthesis of Bubble-Nanorod-Structured Fe₂O₃ Carbon Nanofibers as Advanced Anode Material for Li-Ion Batteries. *www.ascano.org*. 0.1021/acsnano.5b00088

- [22] Cao, J., Wan., Wang, R., Liu, S., Fei, T., Wang, L., and Zhang, T. (2015). Synthesis of core-shell a-Fe₂O₃@NiO Nanofibers with Hollow Structures and Their Enhanced HCHO Sensing Properties. *Journal of Materials Chemistry A*. DOI: 10.1039/c4ta06892k
- [23] Tuharin, K., Turek, Z., Zanáška, M., Kudrna, P., and Tichý, M. (2020). Iron Oxide and Iron Sulfide Films Prepared for Dye-Sensitized Solar Cells. *Materials*. 13. 1797. doi:10.3390/ma13081797
- [24] Ma, J., Guo, X., Yan, Y., Xue, H., and Pang, H. (2018). FeOx-Based Materials for Electrochemical Energy Storage. *Advanced Science*. 5. 1700986. DOI: 10.1002/advs.201700986
- [25] Fang, S., Bresser, D., and Passerini, S. (2019). Transition Metal Oxide Anodes for Electrochemical Energy. *Advanced Energy Materials*. DOI: 10.1002/aenm.201902485
- [26] Li, J., Wen, W., Xu, G., Zou, M., Huang, Z., Guan, L. (2015). Fe-added Fe₃C Carbon Nanofibers as Anode for Li-Ion Batteries with Excellent Low-temperature Performance. *Electrochimica Acta*. 153. 300-305. <http://dx.doi.org/10.1016/j.electacta.2014.12.008>
- [27] Mesa, C.I., Yeisy C., Peralta, Y.M., Hernande, K.V., Antuch, M. Gold, (2020). Silver and Iron Oxide Nanoparticles: Synthesis and Bionanoconjugation Strategies Aimed at Electrochemical Applications. *Topics in Current Chemistry*. (378):12. <https://doi.org/10.1007/s41061-019-0275-y>
- [28] Rodner, M., Puglisi, D., Ekeroth, S., Helmersson, U., Shteplyuk, I., Yakimova, R., Skallberg, A., Uvdal, K., Schütze, A., and Eriksson, J. (2019). Graphene Decorated with Iron Oxide Nanoparticles for Highly Sensitive Interaction with Volatile Organic Compounds. *Sensor*. (19): 918. doi:10.3390/s19040918
- [29] Antarnusa, G., and Suharyadi, E. (2020). Synthesis of Polyethylene Glycol (PEG)-coated Magnetite Fe₃O₄ Nanoparticles and Their Characteristics for Enhancement of Biosensor. *Materials Research Express*. <https://doi.org/10.1088/2053-1591/ab8bef>
- [30] Deng, D., Yu, L., Chen, X., Wang, G., Jin, L., Pan, X., Deng, J., Sun, G., and Bao, X. (2013). Iron Encapsulated within Pod-like Carbon Nanotubes for Oxygen Reduction Reaction. *Angewandte Chemie International Edition*. DOI: 10.1002/anie.201204958
- [31] Palen, E. B., Mendoza, E., Bachmatiuk, A., Rummeli, M.H., Gemming, T., Nogues, J., Skumryev, V., Kalenczuk, R. J., Pichler, T., Silva, S.R.P. (2006). Iron Filled Single-Wall Carbon Nanotubes—A Novel Ferromagnetic Medium. *Chemical Physics Letters*. 421. 129-133. doi:10.1016/j.cplett.2006.01.072
- [32] Kozakova, Z., Kuritka, I., Kazantseva, N. E., Babayan, V., Pastorek, M., Machovsky, M., Bazant, P., and Saha, P. (2015). The Formation Mechanism of Iron Oxide Nanoparticles within the Microwave-assisted Solvothermal Synthesis and Its Correlation with the Structural and Magnetic Properties. *Dalton Transaction*. 44. 21099–21108. DOI: 10.1039/c5dt03518j
- [33] Mu, J., Chen, B., Guo, Z., Zhang, M., Zhenyi Zhang, Z., Zhang, P., Shao, C., and Liu, Y. (2011). Highly Dispersed Fe₃O₄ Nanosheets on One-dimensional Carbon Nanofibers: Synthesis, Formation Mechanism, and Electrochemical Performance as Supercapacitor Electrode Materials. *Nanoscale*. 3. 5034–5040. DOI: 10.1039/c1nr10972c
- [34] Cho, J.S., Hong, Y.J., Lee, J.H., and Kang, Y.C. (2012). Design and Synthesis of Micron-Sized Spherical Aggregates Composed of Hollow Fe₂O₃ Nanospheres for Use in Lithium-Ion Batteries. *Nanoscale*. DOI: 10.1039/C5NR01391G
- [35] Alimin, A., Narsito, N., Kartini, I., Santosa, S.J. (2015). Production of Silver Nanoparticle Chains inside Single Wall Carbon Nanotube with a Simple Liquid Phase Adsorption. *Bulletin of Chemical Reaction Engineering & Catalysis*. 10 (3): 266-274. doi:10.9767/bcrec.10.3.8416.266-274
- [36] Rosmaninho, M.G., Moura, F.C.C., Souza, L.R., Nogueira, R.K., Gomes, G.M., Nascimento, J.S., Pereira, M.C., Fabris, J.D., Ardisson, J.D., Nazzarro, M.S., Sapag, K., Araújo, M.H., Lago, R.M. (2012). Investigation of Iron Oxide Reduction by Ethanol as a Potential Route to Produce Hydrogen. *Applied Catalysis B: Environmental*. doi:10.1016/j.apcatb.2011.11.038
- [37] Melnikov, P., Nascimento, V. A., Arkhangelsky, I. V., Conso, L. Z. Z., de Oliveira, L. C. S. (2014). Thermal Decomposition Mechanism of Iron(III) Nitrate and Characterization of Intermediate Products by the technique of computerized modeling. *Journal of Thermal Analysis and Calorimetry*. 115. 145–151. DOI 10.1007/s10973-013-3339-1
- [38] Kawanari, M., Matsumoto, A., Ashida, R., and Miura, K. (2011). Enhancement of Reduction Rate of Iron Ore by Utilizing Iron Ore/Carbon Composite Consisting of Fine Iron Ore Particles and Highly Thermoplastic Carbon Material. *ISIJ International*. 51(8): 227–1233.

NOMENCLATURE

CNFs	carbon nanofibers
H	high magnification
L	low magnification
LPA	liquid phase adsorption
wt%	percent of weight